Environmental Science and Pollution Research (2023) 30:91617–91635
https://doi.org/10.1007/s11356-023-28818-w

REVIEW ARTICLE

Advances on resource utilization of semi-dry desulfurization ash by thermal decomposition: a high-efficiency and low-temperature method for large-scale processing

Lincheng Liu[1] · Xiaohui Fan[1] · Min Gan[1] · Zengqing Sun[1] · Zhiyun Ji[1] · Jiaoyang Wei[1] · Jiayi Liu[2]

Received: 30 March 2023 / Accepted: 6 July 2023 / Published online: 29 July 2023

Abstract

The semi-dry flue gas desulfurization ash (SFGDA) is an industrial waste generated by the semi-dry desulfurization process, and its resources have been continuously attracted attention. Through the method of heat decomposition, the SFGDA decomposed into CaO and SO_2 has emerged as a prominent research topic. This paper summarizes various of research workers, who revealed that the decomposition temperature of $CaSO_4$ in SFGDA is greater than 1678 K and 1603 K in the air atmosphere and N_2 atmosphere, respectively, presenting challenges such as high energy consumption and limited economic feasibility. On the one hand, the effects of CO and C regulating the pyrolysis atmosphere on reducing the pyrolysis temperature were reviewed. On the other hand, the impact of additives such as Fe_2O_3 and FeS_2 was considered. Ultimately, the joint effects of regulating atmosphere and additives were discussed, and an efficient and low-temperature decomposition route was obtained; adding solid C source and Fe_2O_3 for pyrolysis reaction, the decomposition temperature of $CaSO_4$ can be reduced by at least 230 K and desulfurization efficiency exceeds 95% under the condition of micro-oxidizing atmosphere. Moreover, the CaO resulting from SFGDA decomposition can be further synthesized into calcium ferrite, while the enriched SO_2 can be utilized for the production of industrial sulfuric acid, which holds promising prospects for large-scale industrial applications.

Keywords SFGDA · Thermal treatment · Low-temperature · Decomposition · Circulation reuse

Introduction

SO_2, the primary culprit behind acid rain, poses significant threats to the Earth's ecosystem, human society, and economy, with the steel and electricity sectors being major contributors (Liu et al. 2020; Shi et al. 2017). Given to its severe environmental contamination, SO_2 emission is currently under rigorous regulation by the State Environmental Protection Agency, creating flue gas desulphurization an enormously relevant issue. It is worth noting that the implementation of desulfurization technology in coal-fired power plants and the steel industry has contributed to SO_2 emissions in 2021 accounting for 12.97% of those in 2012, but desulfurized ash will increase proportionately (Wang et al. 2023; Yi et al. 2023), as illustrated in Fig. 1.

The prevailing desulfurization technologies in the current scenario can be categorized into wet desulfurization technology, dry desulfurization technology, and semi-dry desulfurization technology based on the type of desulfurization agent employed (Zhai et al. 2017; Mjalli et al. 2014; Li et al. 2022). However, the dry desulfurization method exhibits significantly lower desulfurization efficiency compared to wet and semi-dry techniques, leading most enterprises to abstain from its adoption. Although the wet desulfurization process achieves a desulfurization effectiveness exceeding 90% (Li et al. 2022), it suffers from drawbacks such as a protracted process flow and the generation of substantial waste liquid and desulfurized gypsum, severely impeding its marketability and utilization. As a result, the conventional desulfurization process is being increasingly replaced by the more advantageous semi-dry desulfurization method, which

Responsible Editor: George Z. Kyzas

✉ Min Gan
ganminhao@126.com

[1] School of Minerals Processing & Bioengineering, Central South University, Changsha, Hunan, People's Republic of China

[2] School of Earth and Space Sciences, Peking University, Beijing, People's Republic of China

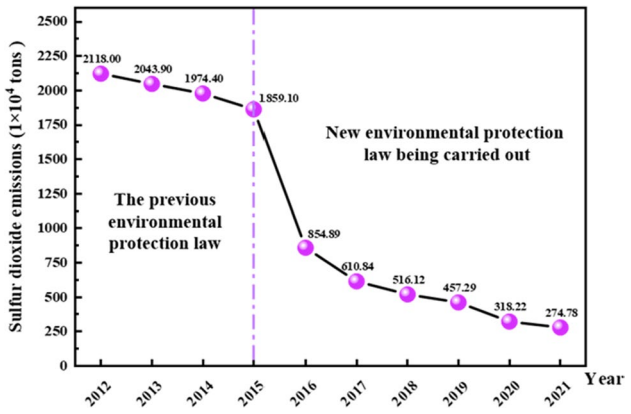

Fig. 1 Sulfur dioxide emissions in China (2012–2021)

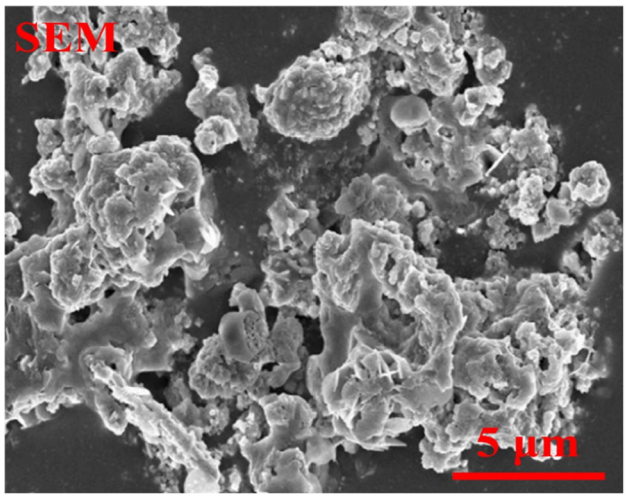

Fig. 2 SEM image of SFGDA from steel factory. (Liu et al. 2010)

entails lower costs and eliminates the generation of excess waste liquid.

Nonetheless, the implementation of the semi-dry desulfurization method by steel mills and power plants gives rise to a considerable quantity of SFGDA, comprising primarily of $CaSO_3$, $CaSO_4$, f-CaO, $Ca(OH)_2$, $CaCl_2$, and $CaCO_3$. (Liang et al. 2011; Zhang et al. 2012; Li et al. 2019). Due to its intricate chemical composition, SFGDA finds limited application in conventional sectors such as cement and building materials, and is predominantly regarded as solid waste, leading to its extensive storage and landfilling. One the one hand, the activated CaO and $CaCl_2$ present in SFGDA negatively impact on the stability and strength of construction materials. The long-term hydration process involving CaO and H_2O generates $Ca(OH)_2$, the $Ca(OH)_2$, which leads to volumetric expansion of buildings and structures. In addition, the presence of deliquescent properties and the release of chloride ions from $CaCl_2$ in SFGDA can cause yellow stains on building walls and corrosion of steel bars, posing a significant threat to building safety.

On the other hand, in accordance with national standards, the mass percentage content of SO_3 in ordinary cement or non-fired bricks should not exceed 3.5 wt.%, restricting the usages of desulfurization ash (Koralegedara et al. 2019; Wang et al. 2005). The prospect of secondary pollution arising from the release of SO_2 from SFGDA under heated or acidic conditions is deeply concerning. Excessive incorporation of SFGDA into building materials is inappropriate, and a substantial amount of unused SFGDA remains stockpiled, thereby necessitating urgent attention to address the utilization of SFGDA.

Recently, the high-temperature pyrolysis process of decomposing $CaSO_4$ and $CaSO_3$ in SFGDA into CaO and SO_2 has garnered significant attention in research. The CaO generated from the pyrolysis of the desulfurization ash is recycled as a calcium source, while the SO_2-rich flue gas undergoes dust removal, washing, and catalytic conversion to produce sulfuric acid, enabling comprehensive utilization of Ca and S in SFGDA. However, the high decomposition temperature of pure $CaSO_4$ reaching 1673 K, poses challenges in practical applications due to elevated production costs and energy consumption. To reduce the decomposition temperature of $CaSO_4$, experts have conducted extensive research using various methods to reduce the decomposition temperature of $CaSO_4$. Currently, there is a lack of comprehensive comparison and evaluation of these methods. Therefore, the primary aim of this review is to summarize recent advancements in the low-energy and low-environmental-risk thermal decomposition of SFGDA. This includes examining the fundamental characteristics of SFGDA, the decomposition behavior of SFGDA in inert, oxidizing, and reducing atmospheres, as well as the effects of solid additives. The present review will serve as a valuable reference for future investigations focused on highly efficient pyrolysis and the subsequent utilization of SFGDA, thereby contributing to the progress of sustainable materials and energy production research.

Physicochemical properties of SFGDA

Wei et al. (Wei et al. 2021) reported that the SFGDA generated by the iron and steel industry exhibits a varied color palette, encompassing shades of pink, light gray, and dark red, attributed to the presence of iron oxide compounds originating from the raw materials employed in the smelting process. Figure 2 depicts SFGDA from a steel industry with an

inconsistent shape, a smooth surface, and an unconsolidated construction (Liu et al. 2010). What is more, the obscuration of SFGDA in steel plants is 15.05%, which is not conducive to apply untreated (Yu et al. 2018).

Furthermore, Liu et al. (2010) confirmed that the particle-size distribution of the SFGDA is from 3.42 to 13.77 μm and the median size is 4.18 μm, shown in Table 1. Surface analysis revealed that the SFGDA possesses a substantial specific surface area of approximately 7940 $m^2 \bullet kg^{-1}$, indicating its pronounced chemical reactivity.

Table 2 presents the composition of semi-dry flue gas desulfurization ash (SFGDA) obtained from steel plants, which includes components such as CaO, $CaSO_3$, $CaSO_4$, f-CaO, SiO_2, Al_2O_3, Fe_2O_3 and MgO. and magnesium oxide (MgO). Furthermore, the SFGDA produced by iron and steel enterprises shows an average content of 32.70 wt.% CaO, 16.81 wt.% $CaSO_3$, and 16.91 wt.% $CaSO_4$, highlighting the abundance of calcium and sulfur resources. Predicated on the thermophysical properties of SFGDA, several studies have been initiated with the thermal decomposition for SFGDA.

Thermal decomposition of SFGDA in inert and oxidizing atmosphere

The elucidation of the thermal decomposition mechanism of carbonate, sulfite, and sulfate compounds is not only intriguing in its own right but also provides valuable insights into the physical and chemical transformations occurring within SFGDA (Yu et al. 2018). Yang et al. (2019a, b) and Zhou et al. (Zhou et al. 2017) discovered that temperature plays a significant role in the decomposition of desulfurization ash under inert or oxidizing conditions. In a nutshell, the thermogravimetric experiment confirmed the existence of five distinct stages during the heating process of SFGDA in an N_2 atmosphere. In reaction stage I, thermodynamic analysis revealed a 2 wt.% reduction in SFGDA at 473 K, attributed to the desorption of adsorbed water and the loss of crystalline water from compounds such as $CaSO_3 \bullet 0.5H_2O$, $CaSO_4 \bullet 2H_2O$.

Consequently, the transformation of $Ca(OH)_2$ into CaO occurred below 673 K. In stage IV, as depicted in Fig. 3 and summarized in Table 3, the thermal decomposition of $CaCO_3$ occurred within the temperature range

Table 1 Particle size characteristic parameters of SFGDA in the steel factory

Indicators	From steel factory	References
Obscuration (%)	15.05	Yu et al. (2018) and Liu et al. (2010)
Median diameter D_{50} (μm)	4.18	
Average diameter size D [4,3] (μm)	5.62	
Average area of track D [3,2] (μm)	1.23	
Shading rate (μm)	24.41	
D25 (μm)	1.53	
D75 (μm)	8.34	
D90 (μm)	13.05	
Specific surface area ($m^2 \bullet kg^{-1}$)	7940	Wei et al. (2021) and Liu et al. (2010)

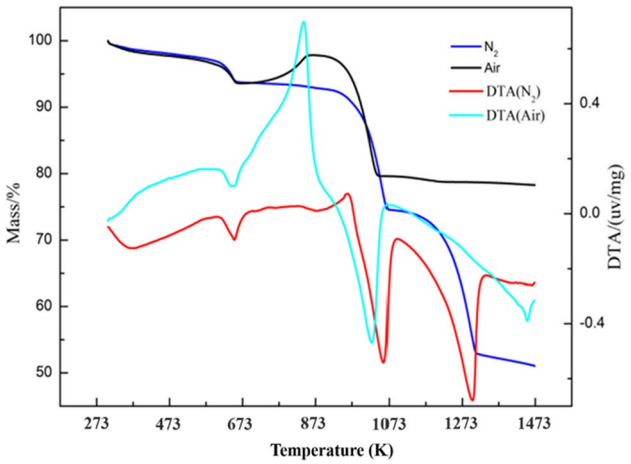

Fig. 3 TGA curves of semi-dry sintering flue gas desulfurized ash in N_2 and air. (Zhou et al. 2017)

Table 2 Chemical characteristics of SFGDA from steel plants. (Liu et al. 2010)

Samples	SiO_2	Al_2O_3	Fe_2O_3	CaO	MgO	$CaSO_3$	$CaSO_4$	f-CaO	LOI
S_1	4.00	2.40	13.60	33.00	2.50	16.90	16.87	Ting	22.50
S_2	3.96	2.38	13.52	32.89	2.49	16.86	16.88	Ting	22.70
S_3	3.93	2.36	13.70	32.86	2.48	16.83	16.90	Ting	22.80
S_4	3.92	2.35	13.64	33.12	2.49	16.80	16.92	Ting	23.10
S_5	3.90	2.36	13.74	32.21	2.47	16.78	16.92	Ting	23.40
S_6	3.87	2.34	13.81	32.14	2.45	16.71	16.97	Ting	23.60

S_1-S_6 are expressed as samples from diffrent steel plants; all values given as percentages; f-CaO, free CaO; Ting indicates that the content of f-CaO is less; LOI, loss on ignition

Table 3 Chemical reaction of SFGDA under different temperature changes

Atmosphere	Stage	T (K)	Reaction equations	Reference
N_2	I	< 473	$CaSO_4 \cdot 2H_2O(s) \rightarrow CaSO_3(s) + 2H_2O(g)$(1) $CaSO_3 \cdot 1/2H_2O(s) \rightarrow CaSO_3(s) + 1/2H_2O(g)$(2)	Yang et al. (2019a, b) Zhou et al. (2017)
	II	< 673	$Ca(OH)_2(s) \rightarrow CaO(s) + H_2O(g)$(3)	Papazian et al. (1972)
	III	953–1073	$CaCO_3(s) \rightarrow CaO(s) + CO_2(g)$(4)	Galan et al. (2013) Narsimhan. (1961)
	IV	1083–1313	$CaSO_3(s) \rightarrow CaO(s) + SO_2(g)$(5)	Zhou et al. (2017)
	V	> 1473	$CaSO_4(s) \rightarrow CaO(s) + SO_2(g) + 1/2O_2(g)$(6)	Yang et al. (2019a, b)
Air	I	< 473	$CaSO_4 \cdot 2H_2O(s) \rightarrow CaSO_3(s) + 2H_2O(g)$(1) $CaSO_3 \cdot 1/2H_2O(s) \rightarrow CaSO_3(s) + 1/2H_2O(g)$(2)	Zhou et al. (2017) Yang et al. (2019a, b)
	II	< 673	$Ca(OH)_2(s) \rightarrow CaO(s) + H_2O(g)$(3)	Papazian et al. (1972)
	III	673–953	$CaSO_3(s) + 1/2O_2(g) \rightarrow CaSO_4(s)$(7)	Chen et al. (1997) Lancia et al. (1997)
	IV	953–1073	$CaCO_3(s) \rightarrow CaO(s) + CO_2(g)$(4)	Castro et al. (2017) Galan et al. (2013) Narsimhan. (1961)
	V	> 1473	$CaSO_4(s) \rightarrow CaO(s) + SO_2(g) + 1/2O_2(g)$(6)	Yang et al. (2019a, b)

of 953–1073 K. Characterized as Fig. 3 and Table 3, the thermal decomposition of $CaSO_3$ in SFGDA commenced around 1083 K and concluded approximately at 1313 K during stage IV. In stage V, the release of SO_2 can be attributed to the minor decomposition of CaSO4 at 1473 K, shown in Table 3. What's more, the decomposition pattern of SFGDA in an N_2 atmosphere exhibits similarities to its calcination in an Ar atmosphere.

The pyrolysis process of $CaSO_3$ in SFGDA also can be divided into five stages in air. Initially, the SFGDA undergoes the release of both free water and structured water below 473 K. Subsequently, $Ca(OH)_2$ decomposes into CaO and H_2O below 673 K. Between 673 and 953 K, the primary reaction observed is the oxidation of $CaSO_3$, resulting in the formation of $CaSO_4$ as the major product. In stage IV, as the temperature range up to 953–1073 K, the CaO and CO_2 will be generated by $CaCO_3$ component in the SFGDA. During stage V, $CaSO_4$ decomposes, yielding CaO and SO_2, which mirrors the reactions observed in an inert atmosphere. In comparison to the former stages, the generation of $CaSO_4$ from $CaSO_3$ in the SFGDA during the oxidation stage is not conducive to low-temperature and high-efficiency decomposition.

Figure 4 (a) illustrates the decomposition efficiency and f-CaO content of $CaSO_3$ in SFGDA following calcination. At 1073 K, in SFGDA undergoes decomposition, resulting in the production of CO_2 and CaO. And then, CaO could rapidly adsorb surrounding SO_2 to synthesize $CaSO_3$, which reduces the decomposition efficiency of $CaSO_3$. The calcined product of SFGDA in an argon atmosphere reveals the presence of CaS between 1073 and 1373 K, indicating the decomposition of calcium sulfite and the formation of CaS and $CaSO_4$. Evidently, achieving comprehensive desulfurization of $CaSO_3$ in an inert atmosphere presents a challenge due to the occurrence of Eq. 8.

$$4CaSO_3(s) \rightarrow CaS(s) + 3CaSO_4(s) \quad (8)$$

Finally, through thermogravimetric non-isothermal experimental research, it was observed that the initial

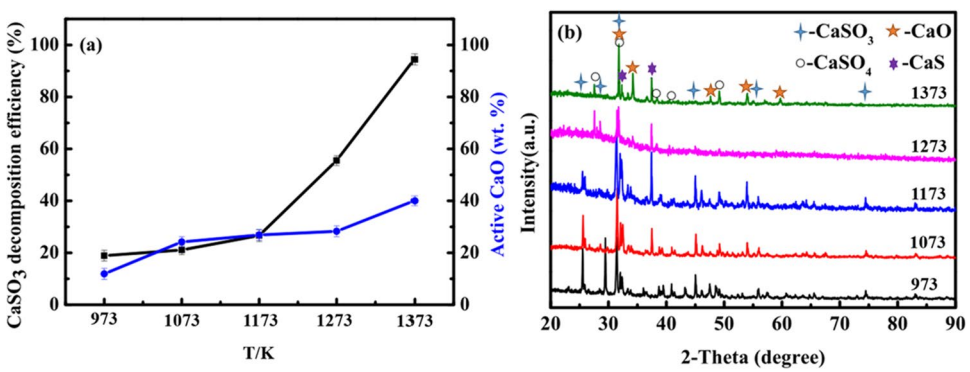

Fig. 4 Effect of temperature on decomposition of SFGDA and phase transition in Ar. (Yang et al. 2019a, b)

decomposition temperature of analytically pure anhydrous $CaSO_4$ powder in a high-purity N_2 atmosphere is 1433 K, while the final decomposition temperature is 1603 K (Ping et al. 2004). Concomitantly, the results indicate that the initial decomposition temperature is 1506 K and the final reaction temperature is 1678 K under an air stream. It is intriguing to note that the prolonged duration of the initial and final reactions is facilitated by an elevated oxygen concentration. Maintaining a specific oxygen concentration in the reaction gas leads to the decomposition of approximately 92 wt.% of $CaSO_4$. As Eq. 5, achieving a higher desulfurization rate poses significant challenges due to the partial coating of CaO on the unreacted $CaSO_4$, thereby impeding the complete decomposition of $CaSO_4$.

Considering the current predicament of incomplete and high-temperature decomposition of $CaSO_4$ in SFGDA, there is an urgent need to reduce the initial reaction temperature for synthesizing CaO with minimal energy consumption. Such an endeavor would signify a noteworthy advancement in the quest for sustainable and energy-efficient methodologies in the production of materials possessing desirable attributes.

SFGDA decomposed by reducing gas

Given the distinctive attributes of SFGDA, a plethora of applications can be envisaged for enhancing gas decomposition processes in the realm of low-temperature pyrolysis. Especially, reducing gas (Robbins 1966; Tian et al. 2010; Yang et al. 2019a, b; Shen et al. 2008; Diaz-bossio et al. 1987; Zheng et al. 2017; Song et al. 2008; Song et al. 2009; Sunphorka et al. 2019; Zhang et al. 2013; Simei et al. 2017), CO is considered to be of particular efficiency to reduce and decompose $CaSO_3$ and $CaSO_4$ to prepare CaO, CaS and SO_2 excellently.

Formation of CaO by reducing gas

In a previous investigation undertaken by Robbins (1966), the adsorption of gas and polymorphic transitions were scrutinized throughout the $CaSO_4$ decomposition process employing reducing gas for CaO synthesis. The production of CaO can be conceptualized as involving dissociation and nucleation phenomena. According to the findings of the adsorption experiments, it was noted that CO does not display notable adsorption onto the $CaSO_4$ surface; instead, it undergoes direct surface reactions. The gaseous CO molecules engage in surface reactions with oxygen molecules present on the $CaSO_4$ surface, resulting in the adsorption and formation of SO_2 and CO_2 compounds on CaO, as depicted in Eq. 9. And then, CO_2 would rapidly desorb into the gas phase, as Eq. 10. The final control step is the direct desorption of SO_2 and the formation of CaO nuclei, as Eq. 11. Once an adequate number of CaO nuclei are formed, the decomposition rate increases. As hypothesized by Robbins (1966), the surface of the CaO core offers a rapid pathway for the desorption of CO_2 and SO_2, facilitating the rapid growth of the nucleus and enhancing the release of SO_2. Thus, the desorption rate is heavily influenced by factors such as gas velocity, particle size, and CO concentration.

$$CO(g) + CaSO_4 \rightarrow CaO \cdot SO_2 \cdot CO_2 \tag{9}$$

$$CaO \cdot SO_2 \cdot CO_2 \rightarrow CaO \cdot SO_2 + CO_2(g) \tag{10}$$

$$CaO \cdot SO_2 \rightarrow CaO + SO_2(g) \tag{11}$$

Conversely, it was observed that the reductive decomposition rate of $CaSO_4$ diminishes as the gas velocity surrounding the particles increases. According to Robbins's proposed mechanism for $CaSO_4$ reduction, it is suggested that a portion of the SO_2 species undergoes reduction to elemental S on the CaO surface, leading to a reduction in the SO_2 concentration at the interface. It is plausible that higher flow rates could contribute to an elevation in the SO_2 concentration on the CaO surface, considering the abundance of SO_2 in the gas stream. The higher concentration of SO_2 on the surface hinders the direct desorption of SO_2 from $CaSO_4$ and the nucleation of CaO. Additionally, decreasing the particle size increases the maximum desulfurization rate of $CaSO_4$, while having no significant impact on the initial desulfurization rate. On the other hand, Robbins (1966) and Wheelock (Wheelock 1960) stated that an increase in CO_2 concentration slightly decreases the maximum desulfurization rate, but does not noticeably affect the initial rate. Furthermore, it is important to maintain a low concentration of CO in the CO-$CaSO_4$ reaction system, as excessive CO concentration is unfavorable for the formation of CaO. Zhao et al. (Zhao et al. 2016) investigated the relationship between SO_2 concentrations, the fraction of released S, and different CO concentrations, specifically 0.10%, 0.25%, 0.50%, and 1.00%, Fig. 5.

The results demonstrated that as the concentration of CO increases, the release of SO_2 occurs earlier, and the amount of sulfur released is directly proportional to the CO concentration. Specifically, under 1.00% CO, more than 21.07% of S was released, approximately double when under 0.25% CO. In a separate study, Okumura et al. (Okumura et al. 2003) investigated the impact of CO concentration (2%, 5%, and 10%) on $CaSO_4$ desulfurization at 1273 K. As Fig. 6(1) shown, it was observed that the initial decomposition reaction rate of $CaSO_4$ increases and the desulfurization rate equilibrium point time of $CaSO_4$ is shortened with an augmentation in the CO concentration. Nevertheless, the desulfurization rate value is diminished by the increase of

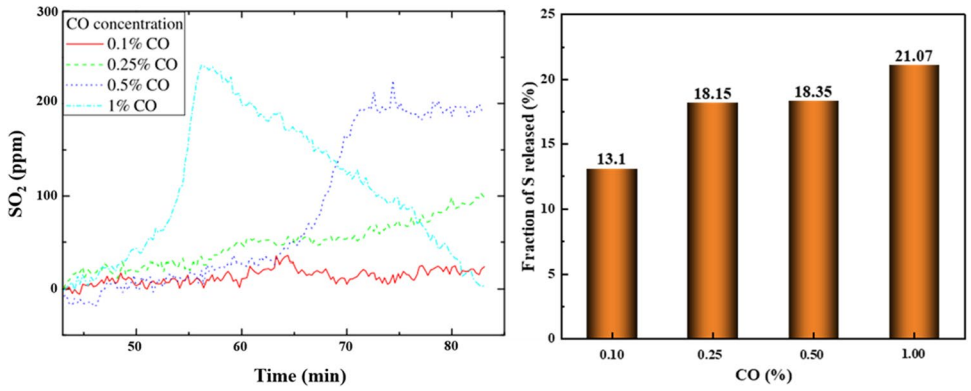

Fig. 5 Effect of CO concentrations on SO_2 concentrations and fraction of S released. (Zhao et al. 2016)

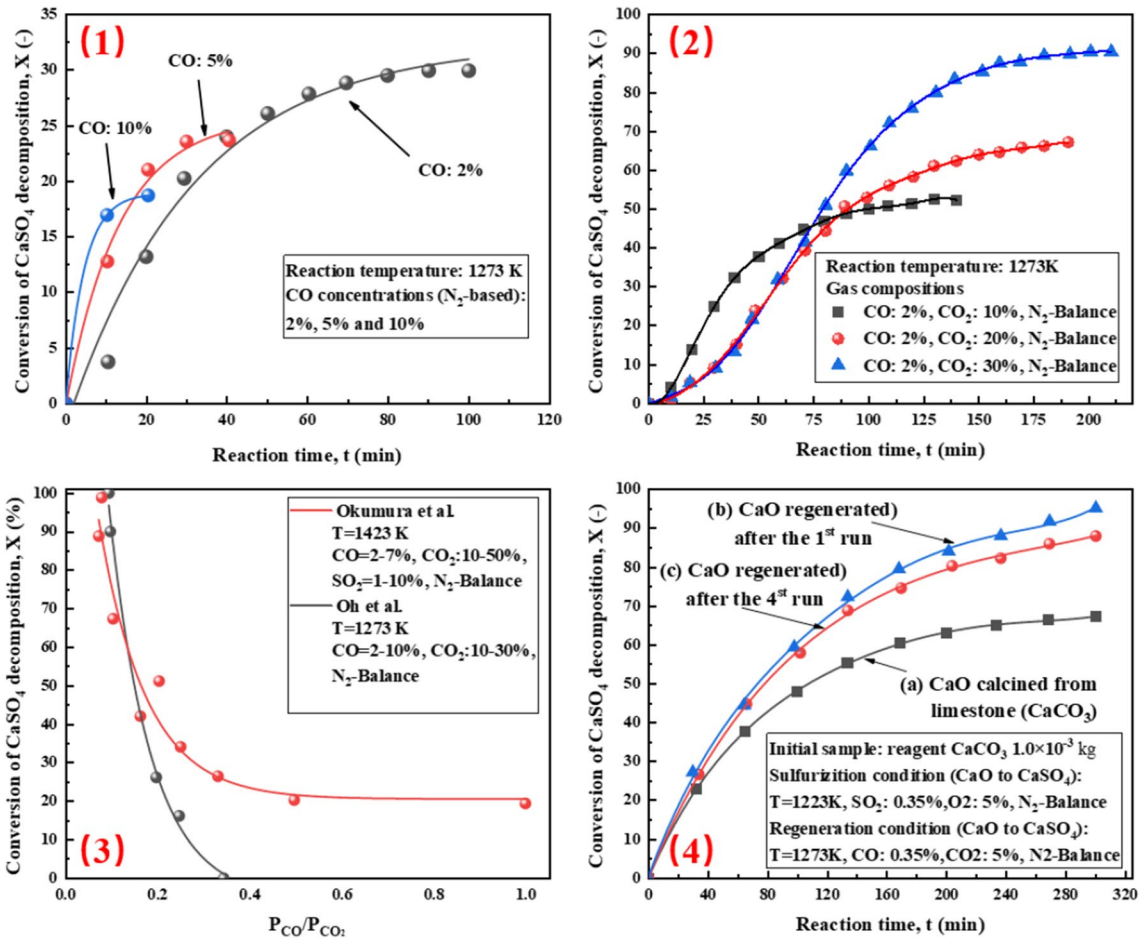

Fig. 6 The effects of CO, CO_2, PCO / PCO_2 and reaction time on desulfurization efficiency: (**1**) effect of the concentration of CO; (**2**) CO_2 on the decomposition of $CaSO_4$ at 1273 K; (**3**) Effect of P_{CO}/P_{CO2} on the final conversion of $CaSO_4$ to CaO; (**4**) Effect of reaction time on $CaSO_4$ decomposition. (Okumura et al. 2003)

CO, implicating low CaO productivity (Zheng et al. 2011a, b; Zhang et al. 2012; Kuusik et al. 1985). the conversion of $CaSO_4$ to CaO is contingent upon the concentrations of CO and CO_2, with a favorable outcome observed when the CO concentration is low and the CO_2 concentration is high. Furthermore, Gruncharov et al. (Gruncharov 1985) and Okumura et al. (2003) have indicated that the initial decomposition rate of $CaSO_4$ decreased when the CO_2 concentration was varied from 10 to 30 vol.% while maintaining a constant CO concentration of 2.00 vol.%. A comparison

between Fig. 6(1) and Fig. 6(2) elucidates that the conversion of $CaSO_4$ to CaO is contingent upon the concentrations of CO and CO_2, with a favorable outcome observed when the CO concentration is low and the CO_2 concentration is high.

By integrating the methodologies employed by Oh et al. (1990) and Okumura et al. (2003), the pseudo-equilibrium desulfurization rate (wt.%) and reduction potential P_{CO}/P_{CO2} are graphed. Figure 6(3) illustrates that as the P_{CO}/P_{CO2} value decreases, the conversion (X) increases. At low reduction potentials ($P_{CO}/P_{CO2} < 0.10$), $CaSO_4$ exhibits near-complete regeneration to CaO. However, discrepancies in the X values are observed, particularly for $P_{CO}/P_{CO2} > 0.2$. These discrepancies may arise due to variations in the reaction conditions employed. Moreover, as depicted in Fig. 6(4), the CaO obtained from the decomposition of $CaSO_4$ demonstrates superior performance in terms of SO_2 and CO_2 re-adsorption compared to the CaO derived from limestone decomposition. At 1273 K, an apparent conversion value of 91% for the decomposition of $CaSO_4$ to CaO was obtained in a 2 vol.% CO and 30 vol.% CO_2 atmosphere.

Irrespective of the reduction reaction of $CaSO_4$ in the CO system, CO-N_2 system, or CO-CO_2-N_2 system, the interaction between CO and $CaSO_4$ resulting in the formation of CaO is accompanied by a highly endothermic reaction. (Kuusik et al. 1985; Gruncharov et al. 1985; Ghardashkhani et al. 1991). The desorption of SO_2 and the formation of CaO necessitate 66 kcal/g·mol, as indicated by Wheelock's (1960) equilibrium measurements. Whereas, the initial reaction between CO and $CaSO_4$, resulting in the production of CO_2 and adsorbed SO_2, releases 27 kcal/g·mol. Therefore, the total heat required for the overall reduction and decomposition of $CaSO_4$ and CO is 39 kcal/g·mol.

In practical engineering applications, incorporating an appropriate quantity of O_2 into the reaction environment can elevate the reaction temperature through the exothermic interaction between O_2 and CO. The introduction of O_2 not only adjusts the partial pressure ratio of CO_2 to CO in the reaction atmosphere but also modifies the reaction mechanism associated with the reduction of CO and the decomposition of $CaSO_4$ into CaO. Xia et al. (Xia et al. 2022) investigated the impact of O_2 on the regeneration process of CaO from $CaSO_4$ through CO reduction. In this investigation, the reduction and decomposition characteristics of $CaSO_4$ were examined and compared under various process conditions in a laboratory-scale fixed-bed reactor utilizing CO-N_2/CO-CO_2-N_2 atmospheres. The results revealed that $CaSO_4$ can be completely decomposed into CaO when the reaction temperature exceeds 1273 K, CO% ≥ 2, and $P(CO_2)/P(CO) \geq 8$. Furthermore, the addition of an appropriate amount of O_2 enhances the yield of CaO in the product. In the O_2-CO-N_2 atmosphere with O_2% of 7 and CO% of 16, $CaSO_4$ can be entirely decomposed into CaO without the need for CO_2 supplementation. The physical properties of CaO produced through the reduction and decomposition of $CaSO_4$ exhibit superior characteristics compared to those obtained through the calcination of $CaCO_3$, which aligns with the conclusions of Okumura (2003).

In addition to the aforementioned factors, Wheelock (1960) investigated the influences of temperature, particle size, gas flow rate, and SO_2 concentration in the gas stream. He concluded that as the temperature increases, the sulfur removal efficiency improves, but accompanied by higher energy consumption, as shown in Fig. 7(a). Moreover, as shown in Fig. 7(b), the maximum desulfurization rates, ranging from 0.1 to 0.3 $lb \cdot s^{-1} \cdot m^{-2}$, exhibited an almost linear increase with the increase of mass velocity in the 2%CO-98%N_2 system. Additionally, as depicted in Fig. 7(c), the initial desulfurization rate showed little dependence on particle size, whereas the maximum desulfurization rate experienced a sharp decline as particle size increased. Hence, it is most probable that the rate is controlled by internal diffusion of the reaction. Eventually, the highest desulfurization rate was achieved at three distinct levels of CO concentration. In Fig. 7(d), it can be witnessed that at a CO concentration of 2%, the maximum desulfurization rate initially decreased with increasing SO_2 concentration from 0 to 0.5%, but subsequently exhibited a slight increase with further increases in SO_2 concentration.

At a CO concentration of 3%, the effect was reversed. And a level of 4%, a different effect was still observed. Although the results are scattered, the maximum desulfurization rate appears to increase slightly with increasing SO_2 concentration across the entire investigated range. A minor concentration of SO_2 in the feed gas exerts a substantial impact on the initial desulfurization rate.

Formation of CaS by reducing gas

Undoubtedly, both reaction temperature and CO concentration have a significant impact on the formation of undesired CaS during the desulfurization process. Wheelock (1960) determined that the decomposition reaction into CaS is negligible at temperatures below 1422 K, but the reaction can be entirely avoided if the temperature reaches 1478 K. In addition, the production of CaS is also suppressed when the P_{CO}/P_{CO2} value in the system is low. To obtain high-purity CaO, it is essential to comprehend the mechanism of CaS generation and manipulate the reaction conditions to minimize its formation. In contrast to the formation reaction of CaO, CaS can be produced when $CaO \cdot SO_2$ continues to react with CO prior to SO_2 desorption.

According to the mechanism of $CaSO_4$ decomposition proposed by Robbins (1966), the most stable intermediate in reductive decomposition is SO_2 adsorbed on CaO, and the adsorbed SO_2 can be reduced to elemental sulfur adsorbed on CaO, Eq. 12.

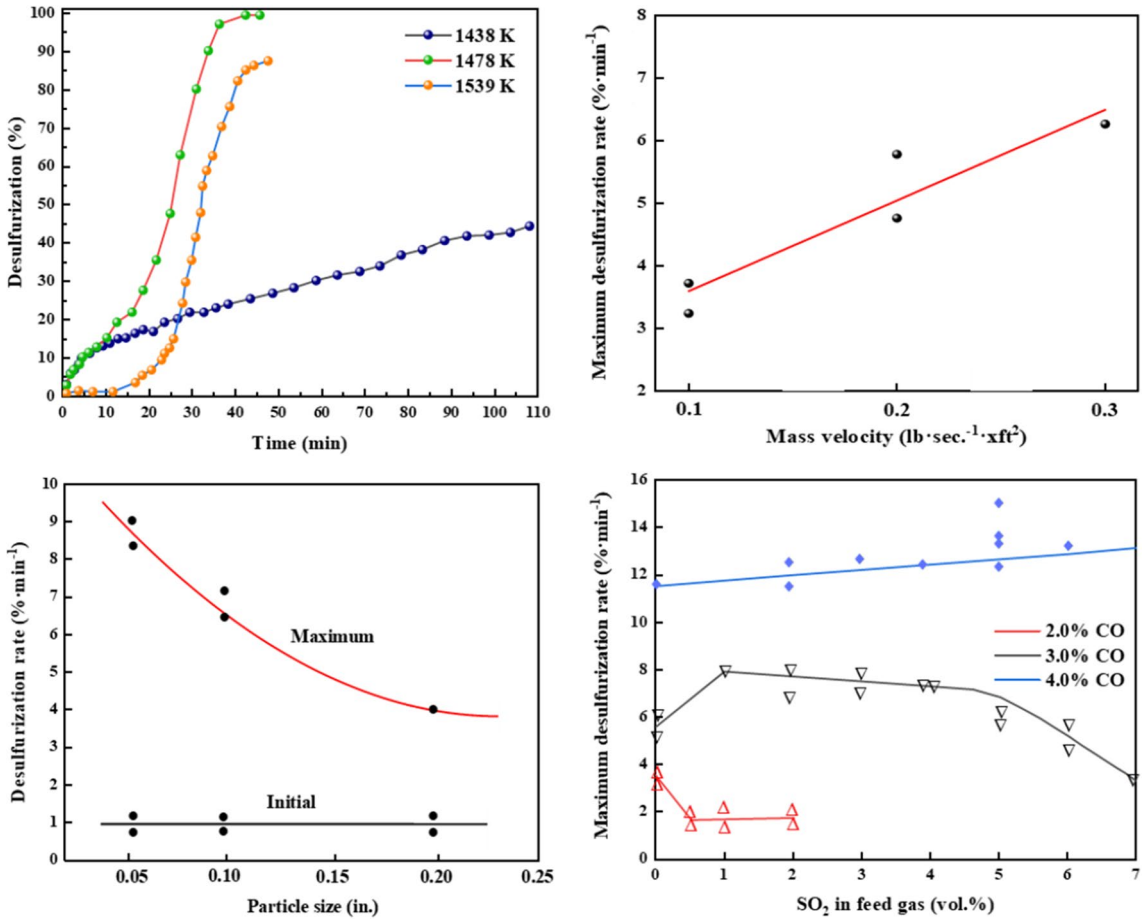

Fig. 7 Effects of temperature, particle size, flow rate and SO_2 concentration in gas stream on $CaSO_4$ desulfurization rate (wt.%). (Wheelock 1960)

$$CaO \cdot SO_2 + 2CO(g) \rightarrow CaO \cdot S + 2CO_2(g) \quad (12)$$

Both Wheelock (1960) and Xia et al. (2022) have demonstrated that at temperatures exceeding 1273 K and with a high concentration of CO_2, CO_2 can displace S on the surface of CaO and be adsorbed. This process effectively hinders the formation of CaS (as described in Eq. 13) by reducing the available amount of adsorbed sulfur for reaction with CO.

$$CaO \cdot S + CO(g) \rightarrow CaS + CO_2(g) \quad (13)$$

SFGDA decomposed by solid reductant

Several researchers have investigated the reductive decomposition of $CaSO_4$ using a solid reductant, including coke (Yan et al. 2014; Kale et al. 1992; Van der Merwe et al. 1999; Ma et al. 2010), lignite (Zheng et al. 2013a, b), charcoal (Chaalal et al. 2020), biomass (Rebbling et al. 2016; Zheng et al. 2011a, b), and graphite (Zheng et al. 2013a, b; Böke et al. 2002; Feng et al. 2019; Ma et al. 2012; Zhou et al. 2011). Presently, there is no universally accepted comprehensive theory that explains the mechanism of thermal decomposition of $CaSO_4$. However, it is recognized that both solid–solid and gas–solid reaction mechanisms are involved in the reduction of $CaSO_4$ to CaO by C.

Formation of CaO by solid reductant

Initial period, it was observed that the decomposition temperature of $CaSO_4$ could be decreased in the presence of coke in the reaction mixture. Figure 8 presented by Factsage 8.1 demonstrates that when delta $G < 0$ kJ•mol^{-1}, the reduction of $CaSO_4$ by C can occur spontaneously, resulting in the production of CaO, CO_2 and SO_2, as shown in Eq. 14. The CO generated from the reaction between C and CO_2 is participated in the decomposition of $CaSO_4$ to CaO at 1200 K approximately, as shown in Eq. 15.

Hence, based on the findings presented in Fig. 8, it can be inferred that the conversion of $CaSO_4$ to CaO and SO_2

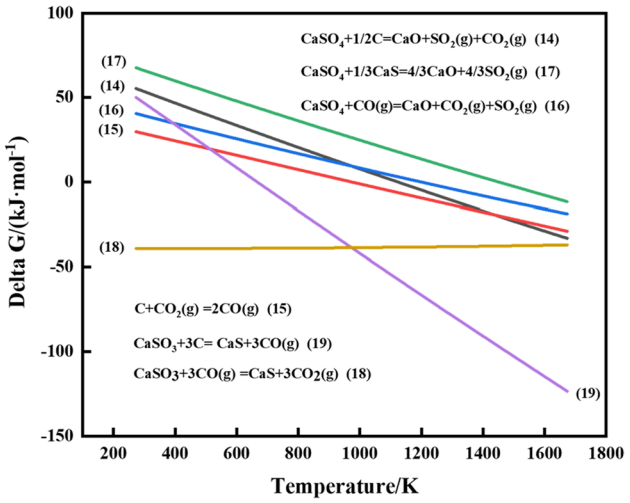

Fig. 8 Delta G – T relationship lines of the major chemical reactions

through C takes places at a higher temperature compared to the decomposition of $CaSO_4$ to CaS, indicating a solid–solid reaction mechanism, as described in Eq. 16. Consequently, at a temperature of 1453 K, the reaction between CaS and $CaSO_4$ leads to the formation of CaO and SO_2, as illustrated in Eq. 17. Moreover, $CaSO_3$ undergoes decomposition to CaS in the presence of C, as demonstrated in Eq. 18.

In accordance with the gas–solid process theory, the initial step involves the oxidation of C to CO, whereupon fully contacts $CaSO_4$ to generate CaO. The reaction between C and $CaSO_4$ do not instantaneously but rather proceeds until completion. Previous studies by Ma et al. (2010) and Su et al. (Su et al. 2019) have highlighted the influence of temperature and C content on the decomposition of $CaSO_4$. Supported by thermodynamic analysis, Ma et al. (2010) determined that the main reaction represented by Eq. 14 could occur within a temperature range of 1273–1423 K. It appears that maintaining a prolonged high temperature and utilizing raw materials with low carbon content, or operating under weak reducing conditions, promotes the decomposition of $CaSO_4$ into CaO. Additionally, Jia et al. (Jia et al. 2016) and Zheng et al. (2011a, b) also investigated the reduction of $CaSO_4$ to CaO using lignite, coal, biomass, and other materials as reducing agents.

To achieve a substantial concentration of SO_2 gas, $CaSO_4$, CaS, S, and FeS_2 can be counted as an abundant sources of sulfur to enhance sulfuric acid production. The interaction between $CaSO_4$ and CaS or S is recognized as a solid-state reaction mechanism, leading to the generation of SO_2 in the gaseous phase. Song et al. (Song et al. 2019) conducted an analysis, affirming the technical feasibility of utilizing FeS_2 as a solid reductive agent in the decomposition of $CaSO_4$ for the production of SO_2. It is noteworthy that the SO_2 capture is not limited to FeS_2 and $CaSO_4$, as $Ca_2Fe_2O_5$ and CaO can also be incorporated into the decomposition slag, thereby enhancing the economic feasibility of the process. The main solid–solid reactions between $CaSO_4$ and FeS_2 are as follows: Eq. 20 and Eq. 21. Significantly, the conducive conditions for obtaining low-sulfur solid products are hindered by the occurrence of Eq. 20. To effectively eliminate residual sulfur from the slag, it is imperative to comprehensively consider the maintenance of an appropriate oxygen pressure within the reaction system.

$$4CaSO_4(s) + 2FeS_2 \rightarrow Ca_2Fe_2O_5(s) + CaO + 5SO_2(g) + CaS(s) \quad (20)$$

$$7CaSO_4(s) + 2FeS_2 \rightarrow Ca_2Fe_2O_5(s) + 5CaO + 9SO_2(g) \quad (21)$$

Formation of CaS by solid reductant

Based on the thermodynamic calculations illustrated in Fig. 8, it can be inferred that the reduction of $CaSO_4$ and $CaSO_3$ to CaS can be accomplished using C and CO at temperatures below 1173 K. Li et al. (Li et al. 2015) revealed that the thermal decomposition of $CaSO_3$ to produce CaS employing coal as a reducer, was carried out with a molar ratio of C to $CaSO_3$ at 2.5 (n(C)/n(S) = 2.5), a reaction temperature of 1173 K, a reaction time of 1.5 h and a coal particle size 100 mesh, shown in Fig. 9. Both thermodynamic calculations and experimental results indicate that the formation of CaS during $CaSO_3$ decomposition can be attributed to Eq. 17 and Eq. 18, involving solid–solid and gas–solid reactions. Additionally, according to Eq. 16, CaS is consumed and reacts with the remaining $CaSO_4$ to produce CaO. XRD and SEM analyses conducted by Li (2015) have validated that CaS is the only solid product formed under appropriate reaction conditions. Consequently, in the reaction system where $CaSO_3$ is reduced by coal with an n(C)/n(S) ratio of 2.5, the decomposition of $CaSO_3$ to CaO can be considered almost negligible.

Analogously, Jia et al. (2016) discovered that the presence of coal significantly enhances the high-temperature decomposition of $CaSO_4$, resulting in the decomposition of 87% $CaSO_4$ into CaS, which is on account of the solid–solid reaction between C and $CaSO_4$. Additionally, the duration of calcination and the particle size of coal influence the decomposition of $CaSO_4$. As indicated in Fig. 9, the decomposition of $CaSO_4$ is more favorable when a reducing agent with an extended reaction time and finer particle size is employed. This observation aligns with the formation reaction of CaS and CaO.

Realistically, an elevation in carbon content tends to promote the formation of CaS, which is unfavorable for sulfur removal. Su et al. (2019) conducted an experimental investigation utilizing a tubular resistance furnace to to explore the influence of carbon content on the desulfurization rate at

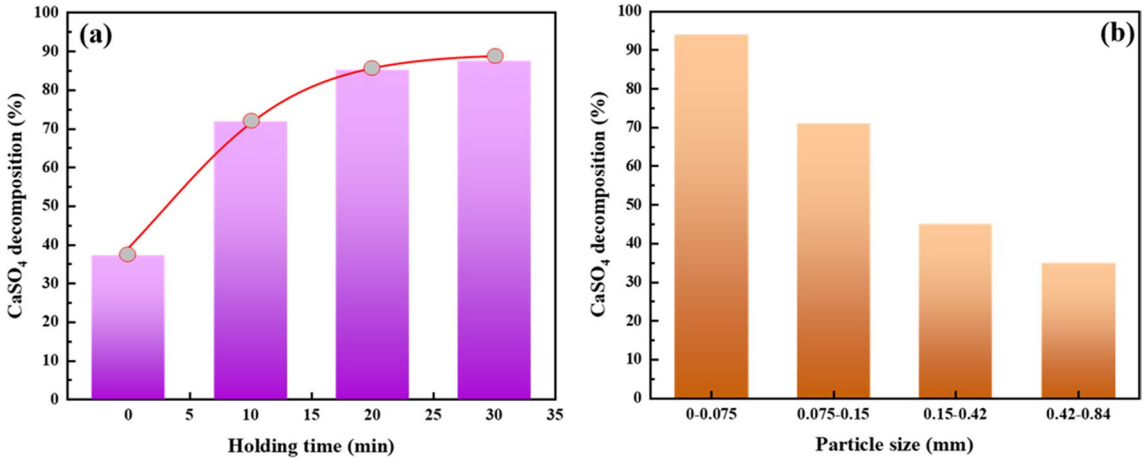

Fig. 9 Effects of holding time and coal particle size on $CaSO_4$ decomposition (Jia et al. 2016)

various temperatures. They observed that an increase in the n(C)/n($CaSO_4$) ratio did not result in an improvement of the desulfurization rate at the same temperature, as depicted in Fig. 10(a). Elevated temperature plays a pivotal role in augmenting the desulfurization rate, as indicated by the reaction mechanism wherein decomposed CaS reacts with $CaSO_4$ to form CaO, and the presence of CO in the gaseous phase accelerates the conversion of $CaSO_4$ to CaO. These two factors are recognized the primary catalysts for improving the desulfurization rate.

Tian, Zheng, and Zhong et al. (Tian et al. 2010; Diazbossio et al. 1985; Simei et al. 2017) have investigated that $CaSO_4$ serves as a promising oxygen carrier, readily reducible to form CaS under high concentrations of CO, while remaining stable in a reducing atmosphere. Within the C-$CaSO_4$ reaction system, the concentration of CO gradually increases as the reaction proceeds, and the potency of the reducing environment is contingent upon the carbon content in the raw material. Furthermore, the conversion rate of $CaSO_4$ and CO into CaS is higher at temperatures below 1273 K compared to their reaction in the solid-state, which results in the production of CaO.

More formidably, the residual of CaS does not contribute to effective sulfur removal in SFGDA, resulting in low CaO production. Therefore, the conversion of CaS to CaO is extremely important to achieve a high desulfurization rate correspondingly. Propitiously, the introduction of O_2 into residual CaS deemed feasible for industrial application, leading to additional CaO generation (Anthony et al. 2003; Turkdogan et al. 1974; Song et al. 2007). The oxidation of pure CaS (with a particle size of 45 μm) was investigated by Davies, Yrjas, and Marban et al. (Davies et al. 1994; Yrjas et al. 1997; Marban et al. 1999) via an atmospheric thermobalance. They observed that the predominant amount

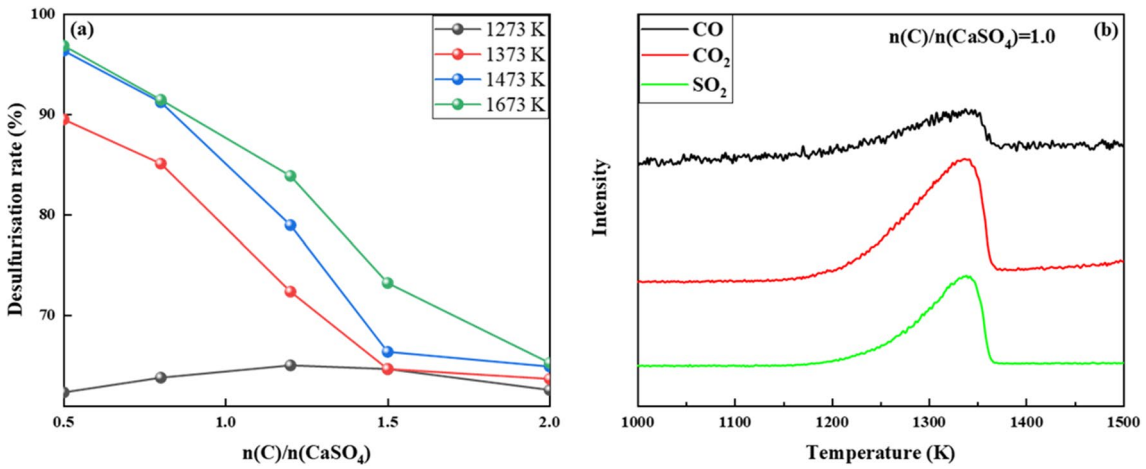

Fig. 10 Variation curve of desulfurization rate with carbon content at different temperatures and gas phase pristine test results. (Su et al. 2019)

of SO_2 was liberated within the initial 25-min period at temperatures ranging from 1123 to 1323 K. Upon oxidizing CaS with 4.2 vol% O_2 for 30 min at 1123 K and 1223 K, the reaction described in Eq. 22 occurred, resulting in $CaSO_4$ conversion rates of approximately 8% and 32%, separately. Meanwhile, the oxidation reaction of CaS and O_2 can be represented by Eq. 23, with corresponding CaO conversion rates of approximately 2% and 30%, respectively. Davies et al. (1994) attributed the release of SO_2 to the apparent solid–solid reaction between CaS and $CaSO_4$, which was confirmed in their study. Furthermore, they discovered that no solid–solid reaction occurred at 1123 K, whereas at 1323 K, complete conversion to CaO was achieved, indicating the transformation from CaS to CaO. Outstandingly, Yrjas et al. (1997) detected that excessively high concentrations of O_2 immediately reacted with CaS, forming impermeable product layers of $CaSO_4$ or CaO, thereby impeding further sulfur release reactions.

$$CaS(s) + 2O_2(g) \rightarrow CaSO_4 \tag{22}$$

$$CaS(s) + 3/2O_2(g) \rightarrow CaO + SO_2(g) \tag{23}$$

Maintaining a moderately low level of O_2 concentration and a temperature greater than 1323 K will benefit the conversion of CaS to CaO (Turkdogan et al. 1974; Song et al. 2007; Wang et al. 2020). Thence, optimizing factors such as the reduced particle size of the SFGDA, thorough mixing of C, maintaining a reaction temperature above 1323 K, and utilizing low C content prove more advantageous in preventing the formation of CaS, thus enabling the production of high-purity CaO.

SFGDA decomposed by compound additive

Apart from solid reductant, solid iron oxides, which are non-reducing agents, also play a significant role in facilitating the decomposition of SFGDA. Higuchi et al. (Higuchi et al. 2016) proposed a method for synthesizing calcium ferrite from waste gypsum board (mainly composed of $CaSO_4{\cdot}2H_2O$) by incorporating iron oxides. Through thermodynamic estimations and small-scale heating tests, three distinct synthetic routes for calcium ferrite were identified: (1) calcium ferrite production in an air environment, (2) single-step heat treatment, and (3) two-step heat treatment, as shown in Fig. 11. The results indicated that calcium ferrite is partially synthesized through the decomposition of the gypsum board in an air atmosphere at 1453 K, but achieving complete decomposition of $CaSO_4$ is exceedingly challenging. Equation 24 is considered the primary reaction, indicating that reducing the P_{O2} or P_{SO2} contributes to the near-complete formation of calcium ferrite.

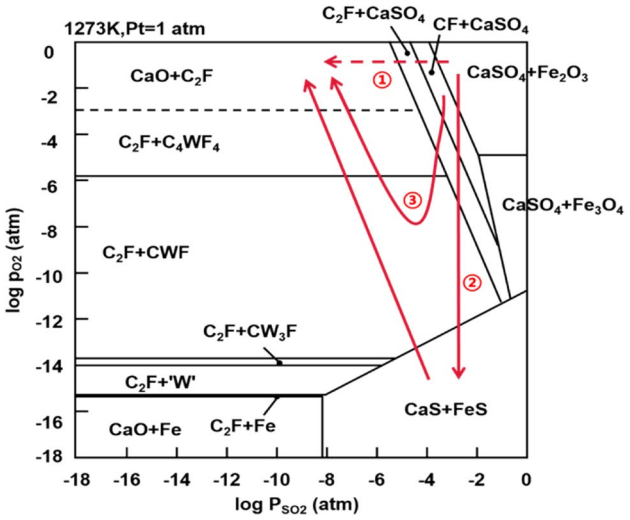

Fig. 11 The phase diagram of chemical equilibrium in the Ca-Fe-S–O system (Higuchi et al. 2016)

$$xCaSO_4(s) + yFe_2O_3(s) \rightarrow xCaO \cdot yFe_2O_3(s) + xSO_2(g) + 0.5xO_2(g) \tag{24}$$

As a consequence, through the addition of C in a specific proportion, the P_{O2} decreases, resulting in desulfation rates of over 95% for $CaSO_4$. Subsequently, there would be more calcium ferrite generated than processes if SO_2 was removed after reaction and slightly oxidative atmosphere in the reaction system was maintained throughout the reaction period (Zhao et al. 2020; Liu et al. 2021). Although some $CaSO_4$ in waste gypsum board decomposes into CaS, it fortunately undergoes oxidation to yield CaO in the presence of trace amounts of oxygen. Whereafter, a portion of the calcium ferrite is produced through the reaction between CaO and Fe_2O_3, as described by Eq. 25 and Eq. 26.

$$CaSO_4(s) + Fe_2O_3(s) + 1/2C(s) \rightarrow CaO \cdot Fe_2O_3(s) + SO_2(g) + 1/2CO_2(g) \tag{25}$$

$$2CaS(s) + Fe_2O_3(s) + 3O_2(g) \rightarrow 2CaO \cdot Fe_2O_3(s) + 2SO_2(g) \tag{26}$$

Actually, Eq. 27 to Eq. 30 demonstrate that carbon would reduce Fe_2O_3 to Fe and simultaneously convert $CaSO_4$ into CaS and CaO. Subsequently, Fe is oxidized to Fe_2O_3 by O_2, which then interacts with $CaSO_4$ to form calcium ferrite.

Meanwhile, C undergoes additional oxidation and is consumed in the processes of iron oxide reduction. Further research on low-carbon consumption is warranted. Gratifyingly, the burning of the C reaction and the oxidation of iron provide a significant amount of energy to the reaction system.

$$3C(s) + Fe_2O_3(s) \rightarrow 2Fe(s) + 3CO(g) \tag{27}$$

$$3CO(g) + Fe_2O_3(s) \rightarrow 2Fe(s) + 3CO_2(g) \tag{28}$$

$$3/2C(s) + Fe_2O_3(s) \rightarrow 2Fe(s) + 3/2CO_2(g) \quad (29)$$

$$CaSO_4(s) + 2Fe(s) + O_2(g) \rightarrow CaO \cdot Fe_2O_3(s) + SO_2(g) \quad (30)$$

To reduce carbon consumption, the two-step heat treatment is considered a reasonable and comprehensive approach. Higuchi et al. (2016) proposes the decomposition of gypsum board with carbon as the first step, leading to the formation of CaO or a small amount of CaS. The second step involves the formation of calcium ferrite from the decomposed material and Fe_2O_3, resulting in the production of calcium ferrite with varying breakdown-product contents. Equation 31 illustrates this process.

$$zCaO(s) + wFe_2O_3(s) \rightarrow zCaO \cdot wFe_2O_3(s) \quad (31)$$

Two distinct processes are present: single-step and two-step processes, with the latter having the potential to reduce carbon consumption theoretically, as depicted in Fig. 12. Furthermore, the two-step process is more advantageous for synthesizing calcium ferrite with low sulfur content compared to the one-step process. Notwithstanding, the two-step process is complicated with high expenses and high facility requirements, and so whether it is environmental protection, energy-saving or economy should be considerately thought in future industrial applications. On the contrary, the one-step production of calcium ferrite involves challenging conditions for precise control of process parameters. Nevertheless, Route ① remains the preferred choice for commercial production due to its straightforward process flow.

Based on the study of Higuchi (2016), calcium ferrite also was prepared from desulfurization gypsum, iron ore, blast furnace dust, and graphite by Zhao (2020). As shown in Fig. 13(a), the raw materials for the reaction were initially introduced into a tube furnace in both powder and block forms, followed by calcination at a temperature of 1373 K under an air atmosphere. It was observed that the powder exhibited a superior desulfurization effect compared to the block form. The decomposition and desulfurization process of $CaSO_4$ involve both solid–solid and gas–solid reactions, with the latter exhibiting significantly faster kinetics than the former. The presence of gaps between the powder particles facilitates the entry of reducing gases such as CO, allowing for gas–solid reactions with $CaSO_4$. Consequently, the use of powdered reactants promotes sulfur removal and leads to a higher desulfurization rate.

It can be seen from the Fig. 13(b) that when the molar ratio of CaO ($CaSO_4$) to Fe_2O_3 is constant, the desulfurization rate of gypsum in argon atmosphere is significantly higher than that in air atmosphere. The sulfur content in the product is lower than that in air atmosphere under argon atmosphere, illuminated that the desulfurization reaction of gypsum hardly occurs in an oxidizing atmosphere. The higher n(CaO): n(Fe_2O_3) contributes to the lower the desulfurization rate of gypsum in argon, which shows that the increase of iron oxide promotes the decomposition and desulfurization of gypsum.

As shown in Fig. 13(c), it is evident that maintaining a constant ratio of n(CaO) to n(Fe_2O_3), a higher carbon content corresponds to a higher desulfurization rate. However, the desulfurization rate shows minimal changes beyond a carbon content of 30%, with the highest achieved rate being approximately 95%. As Fig. 13(d), when the carbon content is fixed and the ratio of n(CaO): n(Fe_2O_3) is 1:1, the product exhibits the highest amount of calcium ferrite, exceeding 95%. Ultimately, the optimal reaction conditions for the one-step synthesis of pure calcium ferrite involve using powdered raw materials in an inert atmosphere, with a CaO/Fe_2O_3 ratio of 1:1 and a carbon content of 30%. To mitigate the presence of CaS and minimize its impact on the desulfurization rate, Zhao et al. (2020) controlled the temperature at 1423 K and utilized the following composition: 30.4 wt.%

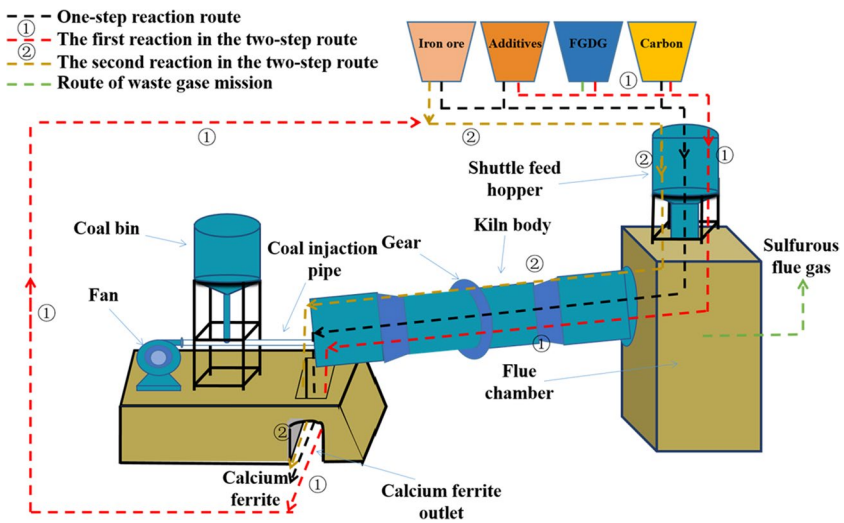

Fig. 12 Diagram of one-step or two-step synthesis of calcium ferrite (Zhao et al. 2020; Liu et al. 2021)

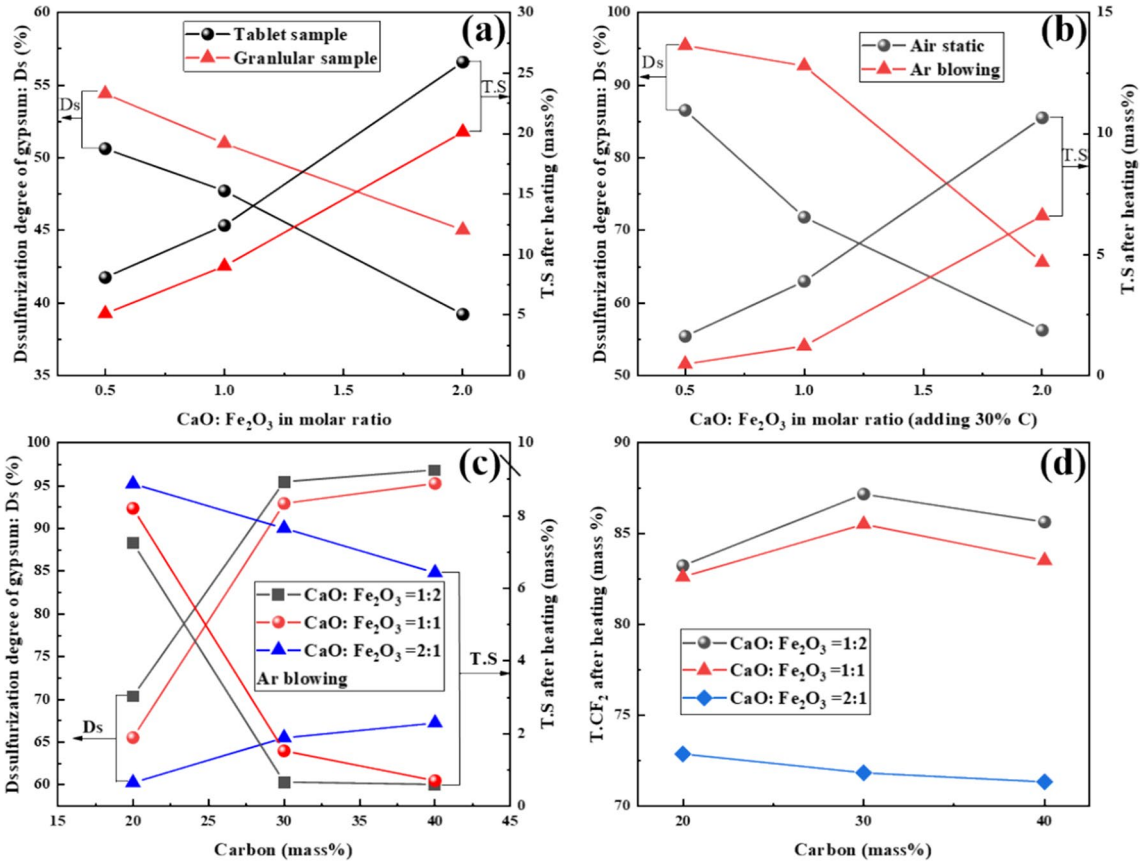

Fig. 13 Curve of desulfurization rate and sulfur content with the ratios of raw materials under different conditions: (**a**) different morphologies, (**b**) different atmospheres, (**c**) different carbon content, (**d**) different iron oxide content. (Zhao et al. 2020)

desulfurization gypsum (with $CaSO_4$ as the primary component), 31.7 wt.% iron ore, 11.1 wt.% blast furnace dust, and 26.8 wt.% graphite. Experimental results demonstrated a significant formation of calcium ferrite under these optimal reaction conditions, resulting in a desulfurization rate of 98.9% and suggesting its feasibility as a recyclable sintering additive.

Summary and perspective

The production of extensively purified CaO and the concentration of SO_2 through pyrolysis are widely acknowledged as promising strategies that have captivated an increasingly large cohort of researchers in their quest to solve the issue of harmless, bulk, and value-added disposal of SFGDA. Achieving efficient and low-temperature sulfur removal in SFGDA necessitates the establishment of favorable reaction conditions. Currently, investigations are underway to optimize the desulfurization efficacy of semi-dry desulfurization ash by controlling variables such as the reaction atmosphere, temperature, reaction duration, and the type and dosage of additives.

SFGDA demonstrates suboptimal pyrolysis efficiency when subjected to temperatures of 1678 K in an air and 1603 K in an N_2, respectively. Furthermore, the presence of $CaSO_4$ significantly prolongs the duration required for complete decomposition of SFGDA, thereby diminishing the desulfurization efficacy of $CaSO_4$ and raising the temperature threshold for sulfur removal. This impedes the large-scale industrial production of CaO and SO_2. Therefore, there is a pressing need to identify a low-temperature, high-efficiency, and environmentally friendly desulfurization additive that enables the recycling of chemical substances such as S and Ca.

As discussed previously (Fig. 14 and Table 4), the decomposition temperature of $CaSO_4$ in the SFGDA can be reduced, leading to an improved desulfurization rate under a reducing atmosphere. In the CO-N_2 atmosphere, the CaS is more effortlessly formed blew 1273 K than CaO generated from SFGDA. This unfavorable occurrence hinders the reduction of sulfur content in solid products. Relatively speaking, there is almost 100% desulfurization rate or decomposition rate in the CO-CO_2-N_2 and CO-CO_2-SO_2-N_2 at 1323–1423 K, but the unalterable truth is that the reduction reaction of $CaSO_4$ with CO is a strongly endothermic

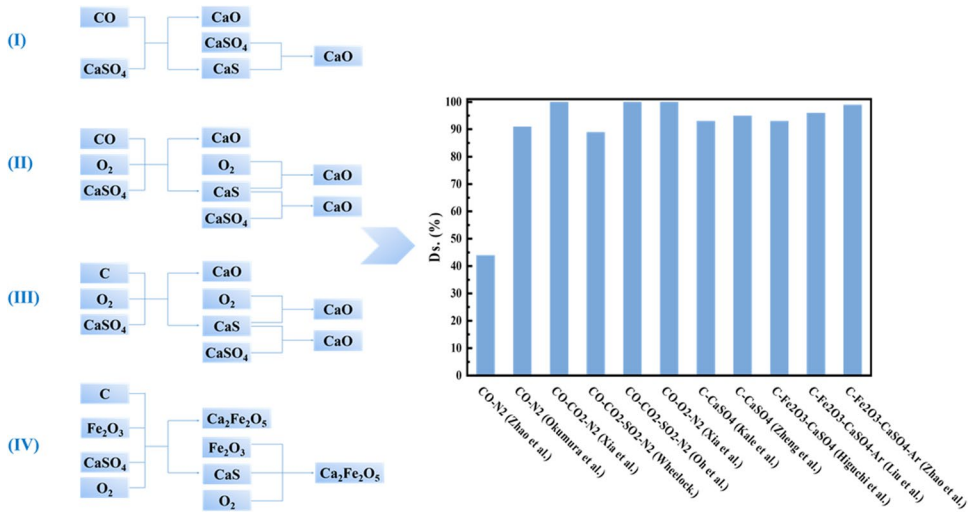

Fig. 14 The synthetic route of CaO and $Ca_2Fe_2O_5$ with various additives

reaction, requiring more external heating. Therefore, in practical industrial applications, it is high-priority to facilitate endothermic reactions through the exothermic reaction between O_2 and CO. What's more, CaS generated from the reduction of $CaSO_4$ can be oxidized by O_2 at 1323–1373 K, reducing residual sulfur and improving desulfurization rate. It is worth noting that the complexity of the system can be simplified by eliminating the presence of SO_2 or CO_2. However, maintaining CO pressure stablely and combustion safely is a tricky issue for industrialization process henceforth.

It is noteworthy that the endeavor to reduce $CaSO_4$ with CO for the production of CaO is currently at the laboratory stage, primarily due to its high raw material cost and expensive equipment investment. In contrast, solid-phase reducing agents such as coke, graphitic carbon, high-sulfur carbon, pyrite, and CaS are more economically viable options for the reductive decomposition of SFGDA. When the molar ratio of $CaSO_4$ to C is 1:0.8, $CaSO_4$ can be effectively decomposed to yield predominantly CaO at temperatures exceeding 1273 K, culminating in a desulfurization rate of over 95%. Additionally, $CaSO_4$ is reduced to form CaO and CaS calcined at 1273 K during the reaction with FeS_2, and Fe_2O_3 is combined with CaO to synthesis calcium ferrite product reused as a sintering additive. The S in the refractory pyrite and SFGDA is migrated to the gas phase, enabling the separation of the sulfur and calcium iron salts. This extraction and utilization of low-grade pyrite not only demonstrates the effective utilization of resources but also holds promising prospects for future applications.

Analogous to sintering flue gas desulfurization gypsum (the main component is $CaSO_4$), the SFGDA decomposition product CaO is combined with Fe_2O_3 to synthesize calcium ferrite using a rotary kiln device (as Fig. 15). Nonetheless, the decomposition temperature of $CaSO_4$ is immobile high, and the desulfurization rate is not satisfactory. By introducing a solid carbon source into the system containing $CaSO_4$ and Fe_2O_3, the optimal decomposition temperature of $CaSO_4$ can be lowered to 1373 K, and the carbon in the reaction system plays the role in providing heat source and reducing agent for the reaction. Within the C-$CaSO_4$-Fe_2O_3 system, $CaSO_4$ is deviously reduced by carbon to form CaS. Moreover, under normal pressure, $CaSO_4$ can be reduced to CaO in a slightly oxidizing atmosphere at a temperature of 1323 K, and then combined with Fe_2O_3 to form calcium ferrite. Therefore, in the C-$CaSO_4$-Fe_2O_3 reaction system, it is crucial to maintain a controlled atmosphere of a mildly reducing atmosphere within the rotary kiln device in order to obtain the calcium ferrite product at a lower temperature.

Notwithstanding, despite the increasing interest in the synergistic preparation of calcium ferrite using calcium sulfate, iron, and carbon-containing solid waste materials, there is a lack of reports on small-scale industrial experiments. What's more, the research on the reaction mechanism of C-$CaSO_4$-Fe_2O_3 involves heterogeneous reactions, including gas–solid and solid–solid reactions, circumlocutionarily complicated. Thus far, there has been no clear mechanistic explanation for the C-$CaSO_4$-Fe_2O_3 reaction system. Furthermore, there is a discrepancy between the results obtained from laboratory experiments and industrial tests, and the scarcity of qualified technical personnel has hindered the industrial application of the semi-dry method. Consequently, further verification and elucidation of the microscopic mechanism underlying the C-$CaSO_4$-Fe_2O_3 reaction are essential to guide actual industrial production. Indispensablely, it is crucial to prioritize the technical training of relevant operators, as it significantly impacts the industrialization process of this method.

Approximately estimated, in the CO-$CaSO_4$-N_2, CO-CO_2-$CaSO_4$-N_2, and C-$CaSO_4$-N_2 reaction systems without oxygen involvement, the reaction temperature is

Table 4 Summary of current research status

Reference	Reactants	Experimental conditions					Evaluation of indicators				
		Shape and particle	Reaction device	Atmosphere	T (K)	t (min)	Solid products	De. (%)	Ds. (%)	Externally heated (Yes or No)	Industrial application situation
Zhao et al. (2016)	$CaSO_4$ and CO	Powder, < 74 μm	Quartz tube furnace heating reactor	N_2	1193	100	CaS CaO	-	44	Yes	Experimental phase
Okumura et al. (2003)	$CaSO_4$ and CO	Powder, 45–63 μm	Double-tube quartz reactor	N_2	1273	100	CaS CaO	30	91	Yes	Experimental phase
Xia et al. (2022)	$CaSO_4$, O_2 and CO	Powder, 30-40 μm	Quartz tube furnace heating reactor	N_2	1323	< 120	CaO	100	100	NO	Experimental phase
Wheelock. (1960)	$CaSO_4$, CO, CO_2, and SO_2	Powder, 2360-2800 μm	A pilot plant scale shaft furnace	N_2	1478	-	CaO CaS	-	89	Yes	Experimental phase
Oh et al. (1990)	$CaSO_4$, CO, CO_2, and SO_2	Disk-shaped pellets, a diameter of 6400 μm and thickness of 7100 μm	Thermogravimetric analysis apparatus	N_2	1423	67	CaO	100	100	Yes	Experimental phase
Jia et al. (2016)	$CaSO_4$ and C	Powder, < 75 μm	A fixed-bed reactor	N_2	1073	30	CaS	94	-	Yes	Experimental phase
Li et al. (2022)	$CaSO_3$ and C	Powder, $CaSO_3$: < 44 μm, Coal: < 150 μm	Muffle furnace	N_2	1173	90	CaS	99		Yes	Experimental phase
Zheng et al. (2017)	$CaSO_4$ and C	Pellets, phosphogypsum: < 74 μm, Coal: < 147 μm,	A tube resistance furnace	N_2	> 1273	-	CaO	-	95	Yes	Experimental phase
Kale et al. (1992)	$CaSO_4$ and C	20000 μm,	A quartz reactor	N_2	-	-	-	-	93	Yes	Experimental phase
Feng et al. (2019)	CaF_2, $CaSO_4$, and C	Powder, phosphogypsum: < 74 μm, Coal: < 147 μm,	A tube resistance furnace	-	1223	60	CaO, CaS	91	35	Yes	Experimental phase
Higuchi et al. (2016)	$CaSO_4$, Fe_2O_3, C	Powder, < 63 μm	A rotary kiln	Ar	< 1473	140	CaO, $Ca_2Fe_2O_5$	-	93	Yes	Small industrial experiments
Zhao et al. (2020)	Fe_2O_3, $CaSO_4$, and C	Powder, < 74 μm	A tube resistance furnace	Ar	1423	240	$Ca_2Fe_2O_5$	> 95	99	Yes	Experimental phase
Liu et al. (2021)	Fe_2O_3, $CaSO_4$, and C	Powder, < 74 μm	A tube resistance furnace	Ar	1373	240	$Ca_2Fe_2O_5$	> 95	96	Yes	Experimental phase

De.(%) indicates the decomposition rate of sulphate, mass %; Ds.(%) indicates the sulphate desulfurization rate, mass %

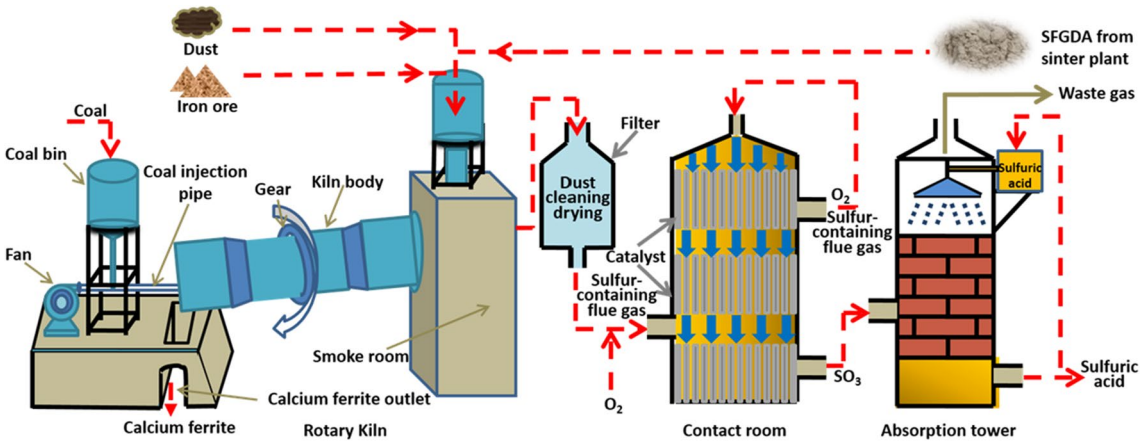

Fig. 15 Industrial flow chart of SFGDA to produce calcium ferrite and sulfuric acid

set at 1100℃, the calcination time is 4 h, and the power of the calciner is 2500 W, resulting in an external energy consumption of approximately 3.6×10^4 kJ, equivalent to 1.10 \$/ton in terms of power cost. Introducing O_2 to facilitate the combustion reaction of CO and coke provides heat for the decomposition of SFGDA, reducing this cost component.

Therefore, coke powder offers a cost advantage as a reducing agent. From a product perspective, if only carbon monoxide or carbon reducing agent is added, and the calcined products of SFGDA are all calcium oxide and sulfuric acid products, the benefits per ton of calcium oxide and sulfuric acid are 72.99 and 58.39 \$/ton. In contrast, the calcium ferrite product obtained by adding carbon and iron oxide to the SFGDA brings a profit of 437.96 \$/ton simultaneously, enabling the comprehensive utilization of calcium, iron, and sulfur resources. Henceforth, the preparation calcium ferrite from SFGDA produced during sintering holds significant potential for multitudinous, innocuous, and high-value consumption of SFGDA, paving the way for its promising commercial application.

Conclusions

Pyrolysis holds great promise as a technology to decompose SFGDA into CaO and SO_2, facilitating the recycling of chemical elements. The purity and properties of the CaO product significantly vary depending on factors such as raw material particle size, composition of the reducing gas, types of additives, calcining temperature, and reaction termination time. In current research endeavors, it is a forefront challenge to achieve high efficiency and low temperature desulfurization for SFGDA to produce CaO at 1273–1373 K within 120 min. Appropriate particle size enhances the desulfurization efficiency of SFGDA, shorten the reaction time and improved the purity of CaO.

(1). SFGDA undergoes decomposition in the presence of reducing gas or a weak oxidizing atmosphere. $CaSO_4$, the main refractory pyrolysis component in SFGDA, can be converted to CaO with a conversion rate of 0.91 in a 2%CO-30%CO_2-68%N_2 atmosphere. Under low reducing atmosphere ($P_{CO}/P_{CO2}\leq0.10$), $CaSO_4$ is completely decomposed into to CaO, but external heat is required for the decomposition process. Interestingly, the adding of 1.0% SO_2 in a CO-CO_2-N_2 ($P_{CO}/P_{CO2}\leq0.10$) the atmosphere achieves a 100% conversion rate of $CaSO_4$ to CaO, and then external heating is needed to provide the required heat for the reaction. Propitiously, it is feasible to attain the necessary reaction temperature by utilizing the exothermic reaction between O_2 and CO, enabling the complete conversion of $CaSO_4$ to CaO in a 7% O_2-16%CO-77% N_2 atmosphere. Unfortunately, there are currently no reports on the industrial application of SFGDA for CaO production CaO due to the high cost of reducing gas, equipment investment, and security concerns.

(2). The addition of solid reducing agents such as C and FeS_2 to SFGDA allows for a decrease in the temperature required for CaO preparation. Besides, these solid additives are more cost-effective compared to reducing gases. While more evidence is required to fully comprehend the precise action mechanism of C on SFGDA, it is recognized that the reaction between C and SFGDA involves solid-solid and gas-solid reactions. When C is added in the ratio of n($CaSO_4$): n(C) = 1: 0.8, the conversion rate of $CaSO_4$ to CaO reaches 95.16% in an N_2 atmosphere above 1273K, resulting in a significant amount of CaO product formation. FeS_2 introduced to a reducing agent, the decomposition temperature of $CaSO_4$ in the SFGDA can be reduced to 1093-1273 K under low-pressure conditions. However, the content of CaS in the solid product is relatively high, and when the temperature is higher than 1273 K, more encouraging to the decomposition of $CaSO_4$ to form CaO.

(3) The addition of iron oxide as an auxiliary agent reduces the decomposition temperature of SFGDA, albeit to a small extent. Therefore, carbon-based reducing agents are often added simultaneously to promote the decomposition of $CaSO_4$, reducing the reaction temperature below 1373K. Under the catalysis of composite additives, CaO can be completely generated, which combines iron oxide to produce calcium ferrite, enhancing the application value of the process. Ultimately, the one-step method of decomposing SFGDA and producing calcium ferrite represents an industrial pyrolysis technology for efficient and economical utilization of SFGDA.

Acknowledgements This work was supported by the National Key R&D Program (No. 2018YFC1900605), China Baowu Low Carbon Metallurgy Innovation Foudation (No. BWLCF202118), and Hunan Province Scientific and Technological Achievements Transformation and Industrialization Program (No. 2020GK4055). We are grateful to these projects for their support.

Author contribution Min Gan, Xiaohui fan and Lincheng Liu contributed to the conception of the study;

Lincheng Liu, Xiaohui fan, Min Gan, Zengqing Sun, Zhiyun Ji performed data collection;

Lincheng Liu, Jiaoyang Wei and Jiayi Liu contributed significantly to graphic drawing;

Lincheng Liu and Min Gan performed wrote the manuscript;

Xiaohui fan and Zengqing Sun helped perform the analysis with constructive discussions.

Funding This work was supported by the National Key R&D Program (No. 2018YFC1900605), China Baowu Low Carbon Metallurgy Innovation Foudation (No. BWLCF202118), and Hunan Province Scientific and Technological Achievements Transformation and Industrialization Program (No. 2020GK4055).

Data availability All data and materials used in this review are publicly available or have been cited accordingly.

Declarations

Competing interests The authors declare no competing interests.

References

Anthony EJ, Jia L, Qiu K (2003) CaS oxidation by reaction with CO_2 and H_2O. Energ Fuel 17(2):363–368. https://doi.org/10.1021/ef020124s

Böke H, Hale Göktürk EH, Caner Saltık EN (2002) Effect of some surfactants on SO_2–marble reaction. Mater Lett 57(4):935–939. https://doi.org/10.1016/S0167-577X(02)00899-6

Castro R, Collins CA, Rago TA et al (2017) Currents, transport, and thermohaline variability at the entrance to the Gulf of California (19–21 April 2013). Cienc Mar 43(3):173–190. https://doi.org/10.7773/CM.V43I3.2771

Chaalal O, Madhuranthakam CMR, Moussa B et al (2020) Sustainable approach for recovery of sulfur from phophogypsum. ACS Omega 5(14):8151–8157. https://doi.org/10.1021/acsomega.0c00420

Chen Y, Wu R, Mori S (1997) Development of a new type of thermogravimetric analyser with a mini-tapered fluidized bed. effect of fluidization of particles on the stability of the system. Chem Eng J 68(1):7–9. https://doi.org/10.1016/S1385-8947(97)00058-2

Cruz MDA, Araújo ODQF, de Medeiros JL (2017) Impact of solid waste treatment from spray dryer absorber on the levelized cost of energy of a coal-fired power plant. J Clean Prod 164:1623–1634. https://doi.org/10.1016/j.jclepro.2017.07.061

Davies NH, Laughlin KM, Hayhurst AN (1994) Twenty-fifth symposium (International) on combustion. Combustion Institute, Pittsburgh, PA. 25(1):211–218

Diaz-bossio LM, Squier SE, Pulsifer AH (1985) Reductive decomposition of calcium utilizing carbon monoxide and hydrogen sulfate. Chem Eng Sci 40(3):319–324. https://doi.org/10.1016/0009-2509(85)85094-6

Feng H, Xie R (2019) Phosphogypsum pyrolysis with mineralization agent under weak reducing atmosphere. IOP conference series. Earth Environ Sci 295:1–6. https://doi.org/10.1088/1755-1315/295/5/052030

Galan I, Glasser FP, Andrade C (2013) Calcium carbonate decomposition. J Therm Anal Calorim 111:1197–1202. https://doi.org/10.1007/s10973-012-2290-x

Ghardashkhani S, Lindqvist O (1991) Some aspects of calcium sulphite reduction with carbon monoxide. Thermochrmlcu Actu 190(2):307–318. https://doi.org/10.1016/0040-6031(91)85258-J

Gruncharov I, Kirilov P, Iv PY et al (1985) Isothermal gravimetrical kinetic study of the decomposition of phosphogypsum under CO-CO_2-Ar atmosphere. Thermochim Acta 92:173–176. https://doi.org/10.1016/0040-6031(85)85845-7

Higuchi K, Gushima A, Ikeda T (2016) Synthesis of calcium ferrite from waste gypsum board. ISIJ Int 56(6):168–175. https://doi.org/10.2355/isijinternational.ISIJINT-2015-317

Ji Z, Guo Y, Chen J et al (2016) Microwave-assisted decomposition of FGD gypsum in the presence of magnetite and anthracite. Chem Pap 70(10):1399–1407. https://doi.org/10.1515/chempap-2016-0071

Jia X, Wang Q, Cen K (2016) An experimental study of $CaSO_4$ decomposition during coal pyrolysis. Fuel 163:157–165. https://doi.org/10.1016/j.fuel.2015.09.054

Jia X, Wang Q, Han L et al (2017) Sulfur transformation during the pyrolysis of coal with the addition of $CaSO_4$ in a fixed-bed reactor. J Anal Appl Pyrol 124:319–326. https://doi.org/10.1016/j.jaap.2017.01.016

Kale BB, Pande AR, Gokarn AN (1992) Studies in the carbothermic reduction of phosphogypsum. Metall Trans B 23:567–572. https://doi.org/10.1007/BF02649716

Kato T, Murakami K, Sugawara K (2012) Carbon reduction of gypsum produced from flue gas desulfurization. Chem Eng Trans 29:1974–9791. https://doi.org/10.3303/CET1229135

Koralegedara NH, Pinto PX, Dionysiou DD et al (2019) Recent advances in flue gas desulfurization gypsum processes and applications-A review. J Environ Manage 251:1–13. https://doi.org/10.1016/j.fuel.2019.115783

Kuusik R, Saikkonen P, Niinist L (1985) Thermal decomposition of calcium sulfate in carbon monoxide. J Therm Anal Calorim 30:187–193. https://doi.org/10.1016/j.fuel.2012.09.086

Lancia A, Musmarra D, Pepe F et al (1997) Model of oxygen absorption into calcium sulfite solutions. Chem Eng J 66(2):123–129. https://doi.org/10.1016/S1385-8947(96)03168-3

Li C, Zhong H, Wang S (2015) Reaction process and mechanism analysis for CaS generation in the process of reductive decomposition of $CaSO_3$ with coal. J Taiwan Inst Chem E 50:173–181. https://doi.org/10.1016/j.jtice.2014.12.032

Li H, Zhang H, Li L et al (2019) Utilization of low-quality desulfurized ash from semi-dry flue gas desulfurization by mixing with

hemihydrate gypsum. Fuel 255:1–8. https://doi.org/10.1007/978-3-642-30445-3_58
Li X, Han J, Liu Y (2022) Summary of research progress on industrial flue gas desulfurization technology. Sep Purif Technol 281:1–19. https://doi.org/10.1016/j.seppur.2021.119849
Liang B, Song C, Sun P (2011) Study on characteristics of semi-dry desulfurization ash from dense flow absorber. In 2011 International Conference on Remote Sensing, Environ Transp Eng, IEEE 4460–4463. https://doi.org/10.1109/RSETE.2011.5965321
Liu RP, Guo B, Ren A et al (2010) The chemical and oxidation characteristics of semi-dry flue gas desulfurization ash from a steel factory. Waste Manage Res 28(10):865–871. https://doi.org/10.1177/0734242X09339952
Liu H, Tan Q, Jiang X et al (2020) Comprehensive evaluation of flue gas desulfurization and denitrification technologies of six typical enterprises in Chengdu. China Environ Sci Pollut r 27:45824–45835. https://doi.org/10.1007/s11356-020-10460-5
Liu LC, Zuo HB, Liu WG et al (2021) Preparation of calcium ferrite by flue gas desulfurization gypsum. J Iron Steel Res Int 28:1357–1365. https://doi.org/10.1007/s42243-021-00571-9
Ma ZJ (2020) High-efficiency conversion and comprehensive utilization technology of semi-dry desulfurization ash. Chin Ceram Soc 2:334–346. https://doi.org/10.26914/c.cnkihy.2020.046789
Ma L, Ning P, Zheng S et al (2010) Reaction mechanism and kinetic analysis of the decomposition of phosphogypsum via a solid-state reaction. Ind Eng Chem Res 49(8):3597–3602. https://doi.org/10.1021/ie901950y
Ma LZ, Cui QF, Guo JM et al (2012) Cold test of circulating fludized bed decomposition phosphogypsum. Adv Mater 295:1160–1163. https://doi.org/10.4028/www.scientific.net/AMR.581-582.1160
Marban G, Garcia-calzada M, Fuertes AB (1999) Kinetics of oxidation of CaS particles in the regime of low SO_2 release. Chem Eng Sci 54(1):77–90. https://doi.org/10.1016/S0009-2509(98)00210-3
Mjalli FS, Ahmed OU, Al-Wahaibi T et al (2014) Deep oxidative desulfurization of liquid fuels. Rev Chem Eng 30(4):337–378. https://doi.org/10.1515/revce-2014-0001
Narsimhan G (1961) Thermal decomposition of calcium carbonate. Chem Eng Sci 16:7–20. https://doi.org/10.1016/0009-2509(61)87002-4
National Bureau of Statistics of China (2021) China Statistical Yearbook. China Statistics Press, Beijing
Oh JS, Wheelock TD (1990) Reductive decomposition of calcium sulfate with carbon monoxide: reaction mechanism. Ind Eng Chem Res 29(4):544–550. https://doi.org/10.1016/0009-2509(85)85094-6
Okumura S, Mihara N, Kamiya K et al (2003) Recovery of CaO by Reductive Decomposition of Spent Gypsum in a $CO–CO_2–N_2$ Atmosphere. Ind Eng Chem Res 42(24):6046–6052. https://doi.org/10.1021/ie0302645
Papazian HA, Pizzolato PJ, Peng J (1972) Observations on the thermal decomposition of some dithionates and sulfites. Thermochim Acta 5(2):147–152. https://doi.org/10.1016/0040-6031(72)85019-6
Ping XH, Jun-hu Z, Yu CXI et al (2004) Experimental Study of Decomosition Behavior of $CaSO_4$ in Different Atmospheres. Power Eng 24(6):889–892
Rebbling A, Näzelius I, Piotrowska P et al (2016) Waste gypsum board and ash-related problems during combustion of biomass. 2. fixed bed. Energ Fuel 30(12):10705–10713. https://doi.org/10.1021/acs.energyfuels.6b01521
Robbins LA (1966) Gas adsorption and polymorphism in the reductive decomposition of calcium sulfate. Iowa State University. https://doi.org/10.31274/RTD-180813-2818
Shen L, Zheng M, Xiao J et al (2008) A mechanistic investigation of a calcium-based oxygen carrier for chemical looping combustion. Combust Flame 154(3):489–506. https://doi.org/10.1016/j.combustflame.2008.04.017
Shi W, Lin C, Chen W et al (2017) Environmental effect of current desulfurization technology on fly dust emission in China. Renew Sust Energ Rev 72:1–9. https://doi.org/10.1016/j.rser.2017.01.033
Simei Z, Min Z, Sixu P et al (2017) Thermodynamics on Sulfur Migration in $CaSO_4$ Oxygen Carrier Reduction by CO. Chem Res Chinese u 33(6):979–985. https://doi.org/10.1007/s40242-017-6457-7
Song Z, Zhang M, Ma C (2007) Study on the oxidation of calcium sulfide using TGA and FTIR. Fuel Process Technol 88(6):569–575. https://doi.org/10.1016/j.fuproc.2007.01.014
Song Q, Xiao R, Deng Z et al (2008) Chemical-looping combustion of methane with $CaSO_4$ oxygen carrier in a fixed bed reactor. Energ Convers Manage 49(1):3178–3187. https://doi.org/10.1016/j.enconman.2008.05.020
Song Q, Xiao R, Deng, et al (2009) Reactivity of a $CaSO_4$-oxygen carrier in chemical-looping combustion of methane in a fixed bed reactor. Korean J Chem Eng 26:592–602
Song WM, Zhou J, Wang B et al (2019) Production of SO_2 gas: New and efficient utilization of flue gas desulfurization gypsum and pyrite resources. Ind Eng Chem Res 58(44):20450–20460. https://doi.org/10.1021/acs.iecr.9b04403
Su H, Zuo HB, Zhao J (2019) Desulphurization of gypsum at high temperature. Inorg Chem Ind 51(7):68–73. https://doi.org/10.11962/1006-4990.2018-0486
Sunphorka S, Kanokwannakorn P, Kuchonthara P (2019) Chemical Looping Combustion of Methane or Coal by $Fe_2O_3/CaSO_4$ Mixed Oxygen Carrier. Arab J Sci Eng 44:5501–5512. https://doi.org/10.1007/s13369-019-03799-6
Tian H, Guo Q, Yue X et al (2010) Investigation into sulfur release in reductive decomposition of calcium sulfate oxygen carrier by hydrogen and carbon monoxide. Fuel Process Technol 91(11):1640–1649. https://doi.org/10.1016/j.fuproc.2010.06.013
Turkdogan ET, Rice BB, Vinters JV (1974) Sulfide and sulfate solid solubility in lime, magnesia, and calcined dolomite: Part I. CaS and $CaSO_4$ solubility in CaO. Metall and Mater Trans B 5:1527–1535. https://doi.org/10.1007/BF02646322
Van der Merwe EM, Strydom CA, Potgieter JH (1999) Thermogravimetric analysis of the reaction between carbon and $CaSO_4{\cdot}2H_2O$, gypsum and phosphogypsum in an inert atmosphere. Thermochim Acta 340:431–437. https://doi.org/10.1016/S0040-6031(99)00287-7
Wang WL, Cui L, Ma CY (2005) Study on properties and comprehensive utilization of dry and semi-dry desulfurization residues. Power Syst Eng 21(5):27–29 (**(In Chinese)**)
Wang Y, Wan T, Zhong Y et al (2020) Environmental sustainability of renewable phosphogypsum by CaS. J Therm Anal Calorim 139:3457–3471. https://doi.org/10.1007/s10973-019-08718-3
Wang YF, Yang T, Ding L et al (2023) Subcritical hydrothermal oxidation of semi-dry ash from iron ore sintering flue gas desulfurization: Experimental and kinetic studies. Waste Manage 160:156–164. https://doi.org/10.1016/j.wasman.2023.02.002
Wei R, Zhu Y, Di Z et al (2021) Impurity removal and hydrothermal heterogeneous cryogenic rapid oxidation of semi-dry desulfurization ash from iron ore sintering flue gas. J Water Process Eng 21(8):951–958. https://doi.org/10.12034/j.issn.1009-606X.220223
Wheelock TD, Boylan DR (1960) Reductive Decomposition of Gypsum by Carbon Monoxide. J Ind Eng Chem 52(3):215–218. https://doi.org/10.1021/IE50603A023
Xia X, Zhang L, Li Z et al (2022) Recovery of CaO from $CaSO_4$ via CO reduction decomposition under different atmospheres. J Environ Manage 30:1–11. https://doi.org/10.1016/j.jenvman.2021.113855
Yan B, Ma L, Ma J (2014) Mechanism analysis of Ca, S transformation in phosphogypsum decomposition with Fe catalyst. Ind Eng Chem Res 53(18):7648–7654

Yang J, Ma L, Yang J (2019a) Chemical looping gasification of phosphogypsum as an oxygen carrier: The Ca and S migration mechanism using the DFT method. Sci Total Environ 689:854–864. https://doi.org/10.1016/j.scitotenv.2019.06.506

Yang Y, Fan Y, Li H et al (2019b) Study on thermal decomposition process of semidry flue gas desulfurization ash. Energ Fuel 33(9):9023–9031. https://doi.org/10.1021/acs.energyfuels.9b02116

Yi DQ, Wang Y, Ye KH et al (2023) Progress in resource utilization of calcium-based semi-dry desulphurization ash in iron and steel industry. Chin J Eng (accepted). https://doi.org/10.13374/j.issn2095-9389.2022.12.23.002.

Yrjas P, Hupa M, Iisa K (1997) Pressurized stabilization of desulfurization residues from gasification processes. Fuel and Energy Abstracts 10(6):1189–1195. https://doi.org/10.1021/ef960013r

Yu YP, Fang Y, Chai SY et al (2018) Properties of semi-dry flue gas desulfurization ash and used for phosphorus removal. IOP Conf Series: Mater Sci Eng 359(1):1–7. https://doi.org/10.1088/1757-899X/359/1/012021

Zhai M, Guo L, Sun L et al (2017) Desulfurization performance of fly ash and $CaCO_3$ compound absorbent. Powder Technol 305:553–561. https://doi.org/10.1016/j.powtec.2016.10.021

Zhang J, Lu P (2012) Study on kinetic parameters and reductive decomposition characteristics of FGD Gypsum. In 7th International Symposium on Coal Combustion (ISCC), Springer Berlin Heidelberg, Berlin, Heidelberg, p 411–417. https://doi.org/10.1007/978-3-642-30445-3_58

Zhang X, Song X, Sun Z et al (2012) Density functional theory study on the mechanism of calcium sulfate reductive decomposition by carbon monoxide. Ind Eng Chem Res 51(18):6563–6570. https://doi.org/10.1016/j.fuel.2012.09.086

Zhang X, Song X, Sun Z et al (2013) Density functional theory study on the mechanism of calcium sulfate reductive decomposition by methane. Fuel 110:204–211. https://doi.org/10.1016/j.fuel.2012.09.086

Zhao S, You C (2016) The effect of reducing components on the decomposition of desulfurization products. Fuel 181:1238–1243. https://doi.org/10.1016/j.fuel.2016.01.090

Zhao J, Su H, Zuo HB et al (2020) The mechanism of preparation calcium ferrite from desulfurization gypsum produced in sintering. J Clean Prod 267:1–10. https://doi.org/10.1016/j.jclepro.2020.122002

Zheng M, Shen L, Feng X et al (2011a) Kinetic model for parallel reactions of $CaSO_4$ with CO in chemical-looping combustion. Ind Eng Chem Res 50(9):5414–5427. https://doi.org/10.1021/ie102252z

Zheng S, Ning P, Ma L et al (2011b) Reductive decomposition of phosphogypsum with high-sulfur-concentration coal to SO_2 in an inert atmosphere. Chem Eng Res Des 89(12):2736–2741. https://doi.org/10.1016/J.CHERD.2011.03.016

Zheng D, Lu H, Sun X et al (2013a) Reaction mechanism of reductive decomposition of FGD gypsum with anthracite. Thermochim Acta 559:23–31. https://doi.org/10.1016/j.tca.2013.02.026

Zheng SC, Cheng FX, Wang ZJ (2013b) Production of SO_2 and lime from phosphogypsum reduced with lignite in a nitrogen atmosphere. Adv Mat Res 803:94–98. https://doi.org/10.4028/www.scientific.net/AMR.803.94

Zheng M, Xing Y, Zhong S et al (2017) Phase diagram of $CaSO_4$ reductive decomposition by H_2 and CO. Korean J Chem Eng 34:1266–1272. https://doi.org/10.1007/s11814-016-0360-7

Zhou MK, Ying GL, Li BX et al (2011) Study on the kinetics of phosphor-gypsum pyrolysis. Adv Mater 306–307:1477–1483. https://doi.org/10.4028/www.scientific.net/AMR.306-307.1477

Zhou J, Ding B, Tang C et al (2017) Utilization of semi-dry sintering flue gas desulfurized ash for SO_2 generation during sulfuric acid production using boiling furnace. Chem Eng J 327:914–923. https://doi.org/10.1016/j.cej.2017.06.180